Journal of Engineering and Computer Sciences
Qassim University, Vol. 15, No. 2, pp. 22-38 (July 2022)

Investigation of Performance Prediction of Blast Loaded Concrete Flexural Members Reinforced with High-Strength Bars

Omar M. Alawad
Department of Civil Engineering, College of Engineering, Qassim University, Buraydah, Saudi Arabia, email address, omar.awwad@qu.edu.sa

(Received 21/01/2024; accepted for publication 19/03/2024)

Abstract. This study investigates the use of high-strength reinforcements (ASTM A1035 Grade 100) instead of conventional reinforcement (such as ASTM A615 Grade 60) in a blast-resistant reinforced concrete flexural member. The stress-strain curve of an ASTM A1035 Grade 100 steel differs from conventional grade 60 steel. Grade 100 steel possesses higher strength and an unclear yield threshold. When designing a flexural member to resist blast loading, its resistance function is typically developed utilizing the Unified Facilities Criteria (UFC 3-340-02) manual. The UFC approach simplifies the behavior of steel reinforcement to an elastic portion up to the yield point, followed by a perfectly plastic plateau. With the absence of a clear yield point in high-strength steel, this simplification may not be well represented. The dynamic performance for flexural concrete members reinforced with high-strength steels is developed using the generalized single-degree-of-freedom (SDOF) system. The SDOF performance generated with the simplified approach is compared with a more realistic resistance function of the system obtained by a computational model established with the virtual work principle and the moment curvature of a section. The results indicated that using the UFC approach for the high-strength steel flexural member may require an adjustment factor in order to reach conservative predictions when the reinforcement ratio is between 0.4% and 2%. The results also illustrated a 50% reduction in the area of steel reinforcement when using grade 100 instead of grade 60, indicating less steel congestion in the high-strength reinforced cross-section.

Keywords: High-strength Reinforcement; Blast Analysis; Flexural Member

1. Introduction

The use of high-strength reinforcement has gained more attention in concrete members. High-strength reinforcement, such as ASTM A1035-Grade 100, has a different stress-strain curve than conventional reinforcement [1]. High-strength steel is considerably stronger than conventional steel reinforcement and has no yield plateau. Using grade 100 steel has several advantages, including reduction of reinforcement congestion in heavily reinforced concrete members, enhanced concrete placement, savings in the cost of labor, reduction of construction time, and better resistance to corrosion in some cases [2]. Due to its behavioral variations compared with conventional reinforcement, several researchers investigated the applicability of using high-strength reinforcement as an alternative to conventional reinforcement in flexural members using the current design code provisions [2–5]. Few studies examined the blast behavior of flexural members reinforced with ASTM A1035-Grade 100 [6,7]. Li and Aoude (2019) [6] showed that using high-strength steel improved the blast capacity and the control of peak displacements. However, the study indicated that the under-reinforced stage and sufficient shear reinforcement should be maintained to avoid brittle and shear failure modes. Li and Aoude (2020) continued tackling the issues of their previous study [6] related to the use of the ASTM A1035-Grade 100 reinforcement in concrete members. The study found that the component detailing, such as the use of compression bars and closely spaced ties, allowed more ductility, thus avoiding brittle failures. Aldabagh and Alam (2020) [4] carried out an extensive review related to the use of the ASTM A1035-Grade 100 bars as a reinforcement. The study also provided a comparison related to the design limitation between the American Concrete Institute (ACI) guidelines, i.e., ACI 439.6R [8] and the AASHTO design specifications [9]. It concluded that further limitations are required to be investigated.

Other types of high-strength reinforcement were examined for blast-resistant flexural members in various researches [10–13]; many of these types are no longer used in practice [6]. Keenan (1963) [10] performed an early study to examine high-strength steel with a yield stress of 90 ksi and indicated that higher blast resistance could be obtained compared to specimens with lower-strength steel. However, the study illustrated that factors such as low reinforcement elongation and excessive deflection under static loading may restrict the use of high-strength steel in blast applications. Thiagarajan et al. (2014) [12] examined various concrete and steel strength grades in reinforced concrete slabs when subjected to blast loadings. The study indicated an improvement in the level of protection for specimens with higher strength for steel and concrete. Li et al. (2015) also indicated in their study that similar improvement for specimens with both concrete and steel that possessed high strength for close-in blast scenarios.

Further investigations are required on predicting the performance of blast-resistant flexural members reinforced with ASTM A1035-Grade 100 rebars when utilizing the simplified approach detailed in the Unified Facilities Criteria (UFC 3-340-02) [14]. Hence, a study is performed to compare the dynamic performance of the simplified approach resistance functions developed utilizing the UFC 3-340-02 [14] with a computational model developed with more realistic resistance functions based on the virtual work principle and moment curvature approach. The dynamic response of the simply supported flexural panels subjected to a blast load is carried out considering the generalized single degree of freedom system (SDOF). The study also compares the performance of the ASTM A1035-Grade 100 reinforcement and conventional reinforcement, i.e., grade 60 reinforcements, when used in flexural members.

2. Methodology and materials

The investigation in this study is performed considering a one-way flexural reinforced concrete member with simply supported boundary conditions and a span length of 12 ft. The cross-section of the member is 12 inches in width and 24 inches in height, as well as 2.5 inches of concrete cover for both sides (Figure 1). The reinforcement ratio was varied using different areas of reinforcement, which are 0.5, 0.75, 1.0, 1.5, 2.5, 3.5, 5.5, 7.5, and 10.5 in^2. It should be noted that similar areas of reinforcement were used at the top, denoted as *As,* and bottom, denoted as *As',* of the member.

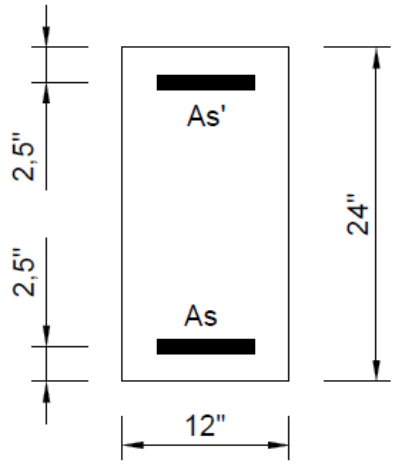

Figure 1: Cross-section details

A simplified triangular blast load was assumed to be applied on the structural member with a peak positive pressure of 200 psi and a duration (*td*) of 10 msec. The applied load is assumed to have no negative pressure phase. The Single-Degree-of-Freedom Blast Effects Design Spreadsheet (SBEDS) tool was used to determine the dynamic response for the examined systems. SBEDS is an Excel-based tool used to design and analyze structural components when subjected to blast loading using an equivalent Single-Degree-of-Freedom (SDOF) system. The equation of motion for the SDOF system is shown in equation (1), where m_e is the mass of the system, K_{LM} is the load-mass transformation factor, $R(y(t))$ is the SDOF system resistance function and $F(t)$ denotes as the history of the blast load. SBEDS utilized a time-stepping method to solve equation (1) and then display the displacement history, $y(t)$. Typically, the maximum displacement occurs at the initial oscillation of the system; hence, the damping term is neglected in this study. The maximum displacement, Δ_{max}, of the response history can then be correlated with the support rotation, θ, which is typically linked to the level of protection as demonstrated in the US Army Corps of Engineers (USACE) [15]. The support rotation can be calculated using equation (2) shown in Figure 2.

The load-mass factor, K_{LM}, is considered an adjustment factor to transform the mass distribution and the applied load along the span of the real structural system into an equivalent SDOF system [16]. The K_{LM} corresponds to the ratio of the mass factor, K_M, to the load factor, K_L. These factors are derived following equations (3) and (4) by considering the shape function, $\phi(x)$, and the length, L, of the real system. The shape function depicts the static deflected shape of the system under an applied load. For a simply supported flexural member under a uniform loading, the K_{LM} factors utilized in the SDOF system are 0.78 and 0.66 during the elastic and plastic response, respectively.

The resistance function, R(y(t)), defines the deformation changes of a structural element as the applied load increases. A structural element's load-deformation (or resistance-deformation)

relationship can be calculated based on material characteristics, geometric configurations, and applied loading conditions. The relationship can be idealized as an elastic-plastic response for a determinate flexural element. On the other hand, for an indeterminate flexural element, the resistance function can be idealized as an elastic-elastoplastic-plastic response. More details on determining the resistance function are explained in sections 2.1 and 2.2.

$$K_{LM}\, m_e\, y''(t) + R\big(y(t)\big) = F(t) \tag{1}$$

$$\theta = \tan^{-1}\left(\frac{\Delta_{max}}{0.5\, L}\right) \tag{2}$$

$$K_M = \frac{1}{L}\int_0^L [\phi(x)]^2\, dx \tag{3}$$

$$K_L = \frac{1}{L}\int_0^L \phi(x)\, dx \tag{4}$$

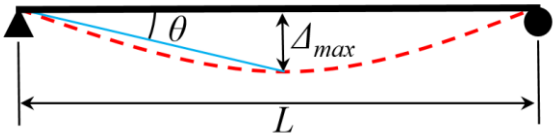

Figure 2: Support rotation of flexural member

Designing a reinforced concrete structure to withstand blast load is one of the main focuses of the UFC 3-340-02 manual. The UFC 3-340-02 presented a methodology to calculate a simplified resistance deflection function for a structural member when subjected to a dynamic load, i.e., will be called "the UFC approach" in this paper. Thus, the UFC approach was used to determine the simplified resistance function for the given cross-section. In addition, another approach has been used to capture a more realistic behavior for a flexural member under uniform loading, considering the moment curvature of the section and the principle of virtual work. The two approaches are utilized to calculate the resistance function for the flexural reinforced concrete member, which is explained below.

2.1 Computational model

A computational model was built using Mathcad software to describe realistic resistance-deflection functions for structural flexural members, considering the virtual work principle and the moment curvature relationship. The virtual work approach or unit-load approach was developed by John Bernoulli in 1717 [17]. The approach is utilized to obtain the displacement or slope at a given location on a structure. The moment curvature can describe the nonlinear capacity of a structural member under bending deformation, considering the nonlinear properties of the concrete and steel reinforcement materials. It is important to note that the computational model accounts for flexural deformation only, while shear deformation is not incorporated. This limitation

highlights the need for future research that accounts for shear and flexural deformation in blast-resistant structural members.

The concrete properties used in the model include a density of 150 pcf and a compressive strength, *f'c*, of 4 ksi. To represent the performance of the concrete material in the compression zone of the section, a stress-strain (f_c-, ε_c) relationship was used as per Hognestad (1952) [18] and represented in equations (5) and (6). Equation (5) is used where the strain is below the strain value, ε_0, that corresponds to the peak stress, assumed here as 0.002. Beyond this limit, equation (6) was used to represent this portion, where *Z* is a constant and was assumed to be 150. The stress-strain relationship for concrete is shown in Figure 3. It should be noted that the Dynamic Increase Factor (DIF) was included in the study to consider the strain rate effect for concrete due to blast loading, corresponding to 1.19, according to the UFC 3-340-02 (2014) [14].

$$f_c = f_c' \left[2\left(\frac{\varepsilon_c}{\varepsilon_0}\right) - \left(\frac{\varepsilon_c}{\varepsilon_0}\right)^2 \right] \tag{5}$$

$$f_c = f_c' \left[1 - \frac{Z}{1000}\left(\frac{\varepsilon_c - \varepsilon_0}{\varepsilon_0}\right) \right] \tag{6}$$

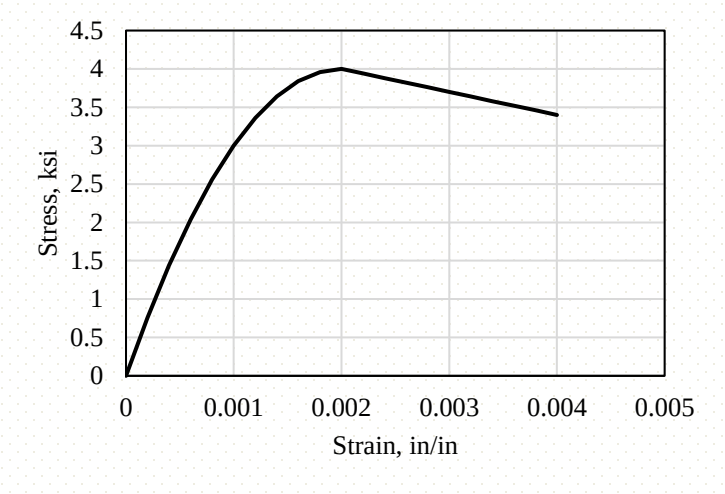

Figure 3: Stress-strain relationship for concrete

The steel reinforcements used in this study, i.e., ASTM A1035-Grade 100 and conventional grade 60 steel, possess different properties. ASTM A 1035-Grade 100 has a smooth stress-strain curve with a minimum tensile strength of 150 ksi and a minimum yield strength, f_y, of 100 ksi that was found by 0.2% offset (Figure 4) [1]. The stress-strain (f_s-ε_s) relationship for ASTM A1035-grade 100 that was used in this approach was developed by Mast et al. (2008) [2] as shown in equations (7) and (8). The modulus of elasticity for grade 100 is similar to that of conventional steel, which has 29000 ksi. The stress-strain relationship for grade 60 is shown in Figure 4 with a yield stress, f_y, and a strain of 60 ksi and 0.00207, respectively. Figure 4 also shows the simplified stress-strain curve with elastic-perfectly-plastic behavior typically recommended by the design codes. The DIF of 1.17 for grade 60 was utilized in the analysis, according to the UFC 3-340-02 [14]. A DIF of 1.0 was assumed for grade 100 steel.

$$f_s = 29000\varepsilon_s \ (ksi) \qquad \varepsilon_s \leq 0.00241 \tag{7}$$

$$f_s = 170 - \frac{0.345}{\varepsilon_s + 0.00104} \ (ksi) \qquad 0.00241 < \varepsilon_s \leq 0.06 \tag{8}$$

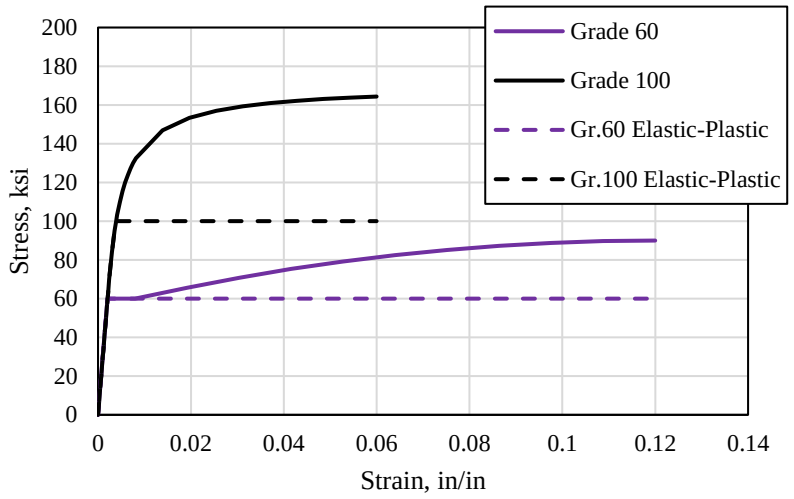

Figure 4: Grade 100 and grade 60 stress-strain curves

The computational model initially finds the moment curvature for the cross-section of the flexural member, with at least 15 points recorded (Figure 5). The flexural member is then discretized uniformly along its length, *L*, where 18 nodes were utilized. Then, a load, w_i, is applied at each node to resemble a uniform load shape and increased for each increment, *i*. The bending moment value, M_i, of each node and increment along the member is determined using equation (9). Similarly, the curvature at each node, $\emptyset_i$, is calculated considering the established moment curvature relationship obtained earlier. Figure 6 summarizes the formation of the structural member's curvature diagram for each increment. Figure 7 shows the curvature distribution along the member for different loading increments, where the dashed line clearly shows the plastic deformation on the mid-span region of the member at a higher loading application.

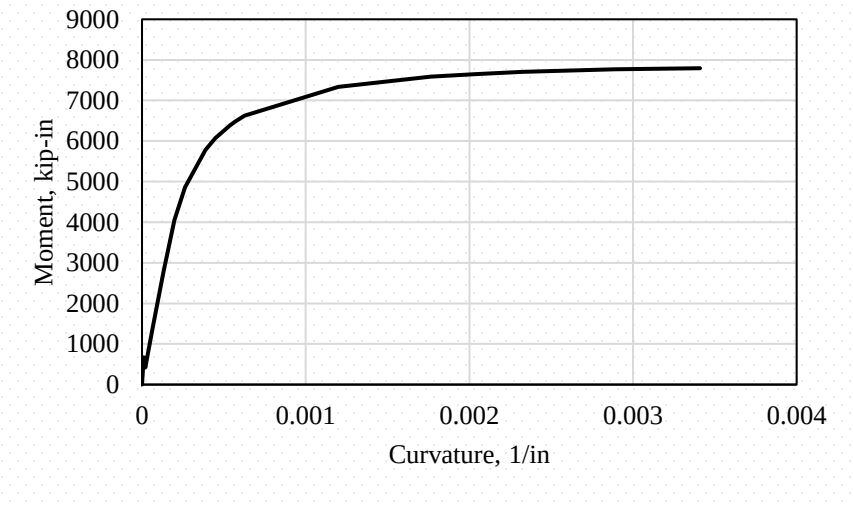

Figure 5: Moment curvature of a reinforced concrete member with grade 100 steel (As= 2.5 in^2)

$$M_i = \left(\frac{w_i \times L \times x}{2} - \frac{w_i \times x^2}{2}\right) \tag{9}$$

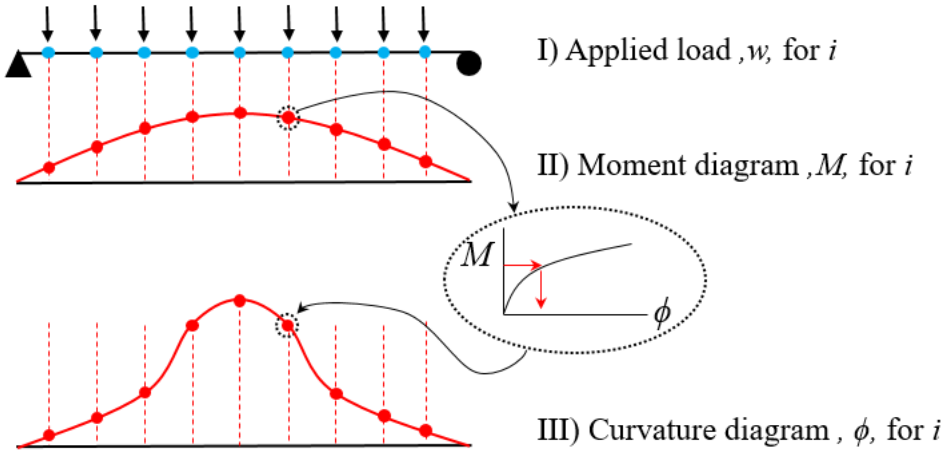

Figure 6: Schematic of curvature diagram development for a load increment

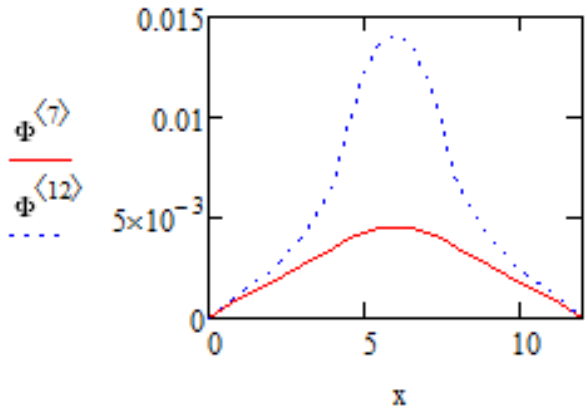

Figure 7: Curvature of a reinforced concrete member with grade 100 steel along the span (As= 2.5 in$^{2)}$.

The maximum deflection of the examined member is then obtained by applying a virtual unit load on mid-span and obtaining the moment diagram along the member $m(x)$. The displacement (Δ_i) of the member at the mid-span for each increment is calculated numerically using equation (10). Following these steps, the resistance function for a structural member is created by relating the applied uniform load with its corresponding maximum deflection for each increment (Figure 8).

$$\Delta_i = \int_0^L \emptyset(x)_i \times m(x)\, dx \tag{10}$$

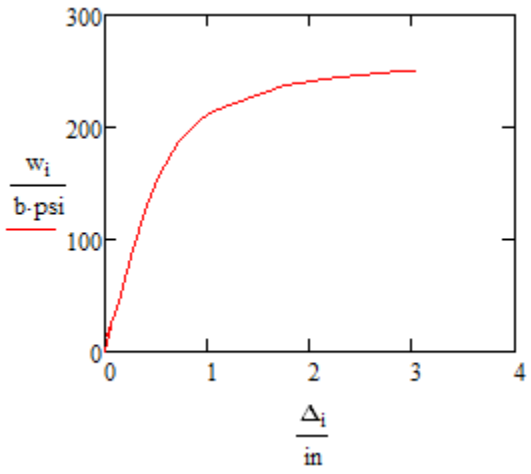

Figure 8: Resistance function of a reinforced concrete member with grade 100 (As= 2.5 in^2)

2.2 The UFC approach

The UFC approach provided three types of reinforced concrete cross-sections based on the blast magnitude and permissible deformation. The three types are 1) Type I considers no spalling for concrete cover over both layers of reinforcement, 2) Type II considers spalling on one side of concrete covers, and 3) Type III assumes spall occurs on both sides of concrete covers. UFC 3-340-02 [14] recommends utilizing Type I when support rotations are less than 2 degrees and Type II when support rotations are larger than 2 degrees but less than 6 degrees.

The resistance function of a simply supported reinforced concrete member using the UFC approach possesses an elastic-perfectly plastic behavior. Two types of cross-sections were used based on the performance of the examined cases in the study, which are Type I and Type II. The ultimate dynamic resisting moment for the one-way flexural member is given by equations (11) and (12) for Type I and equation (13) for Type II. The resistance function's elastic portion of the system will ideally increase with an elastic stiffness slope until yielding displacement, where the ultimate resistance is reached. In the plastic portion of the resistance function, the ultimate resistance of the system is considered to be constant, while an increase in deflection occurs as the applied load continues on the element. The resistance function can be defined considering the ultimate resistance, elastic stiffness, and yield displacement, which are presented in equations (14), (15), and (16), respectively. The elastic-perfectly plastic behavior is considered for steel reinforcement when using the UFC approach, as shown in Figure 4. It is important to note that a realistic stress-strain curve for grade 100 steel has no yield plateau; thus, yield stress cannot be read from the chart directly as in conventional steel. Therefore, the 0.2% offset method was used to define the yield stress and displacement for the high-strength steel. Beyond the 0.2% yield point, the stress is considered to be constant.

$$M_u = \frac{f_{ds} \times A_s}{b} \times (d - \frac{a}{2}) \quad (11)$$

$$a = \frac{f_{ds} \times A_s}{0.85 \times f'_{dc} \times b} \quad (12)$$

$$M_u = f_{ds} A_s \frac{d_c}{b} \quad (13)$$

Where;

a= depth of equivalent rectangular stress block

A_s= area of tension reinforcement

d= distance from extreme compression fiber to centroid of tension steel

d_c= distance between the centroid of the compression and tension steel

b= width of the compression face

f_{ds}= dynamic design stress for reinforcement

$f'dc$= dynamic ultimate compressive strength of concrete

$$r_u = \frac{8M_u}{L^2} \quad (14)$$

$$K_e = \frac{384EI}{5L^4} \quad (15)$$

$$\Delta_e = \frac{r_u}{K_e} \quad (16)$$

Where;

M_u = ultimate moment capacity

r_u= ultimate resistance

K_e= Elastic stiffness

Δ_e= Yield displacement

L = member span length

I = average moment of inertia for gross and cracked section

E = modulus of elasticity

3. Results and Discussion

When an explosion occurs, the structure must have sufficient internal resistance to survive the explosion event. The resistance-deflection relationships for each system were found using the computational model and the UFC approach. These relationships were imported manually into SBEDS using the "General SDOF analysis" type to determine the responses for the systems. SBEDS can also be used to analyze various component types, such as the "reinforced concrete beam or beam-column" type. When selecting this type, the resistance function will be generated by SBEDS after the user defines the geometries and properties of the reinforced concrete member. The user can also insert the blast loading history, and then SBEDS will derive displacement history. The "reinforced concrete beam or beam-column" type in SBEDS can deal with conventional steel with a defined yield point, such as grade 60 steel, when used for reinforced concrete. The resistance function of a reinforced concrete member using grade 100 steel has a smooth curve; hence the "General SDOF analysis" type in SBEDS can be used to derive the response of the system. It should be noted that SBEDS has limited inputs when inserting the resistance function in the "General SDOF analysis" type. Thus, four points from the smooth resistance-deflection curve of specimens with grade 100 steel were selected and inserted into the program.

Considering the selected loading in the study, displacement histories are obtained from the SBEDS spreadsheet for the selected cases, as shown in Figure 9. The support rotation is then calculated using equation (2), considering the maximum displacement of the system. For example, the case with a reinforcement ratio of %0.39, shown in Figure 9, possesses a maximum displacement of 2.23 in, and the support rotation was calculated as 1.77 degrees. The results in this study are generally presented considering the support rotation results versus the selected reinforcement ratio. For example, Figure 10 illustrates the support rotation results for the flexural member with grade 60 steel using the UFC approach versus the analyzed reinforcement ratios. The results for all examined cases indicate a decrease in support rotation for the flexural member while increasing the reinforcement ratio due to the increase in stiffness and capacity of the member.

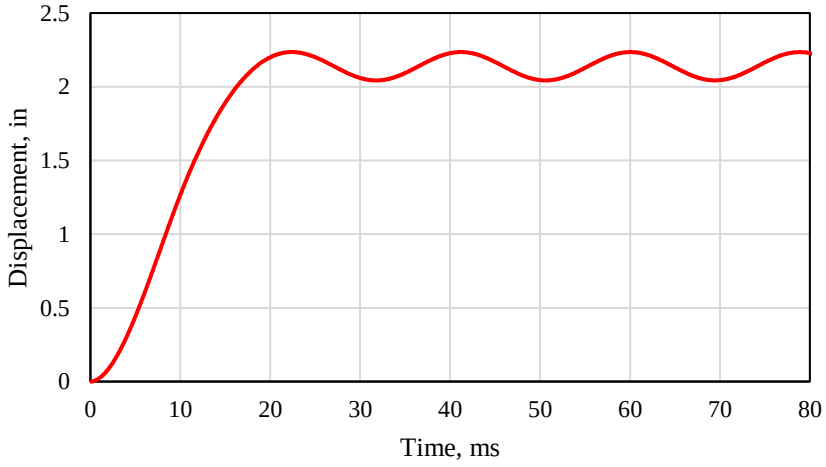

Figure 9: Displacement history

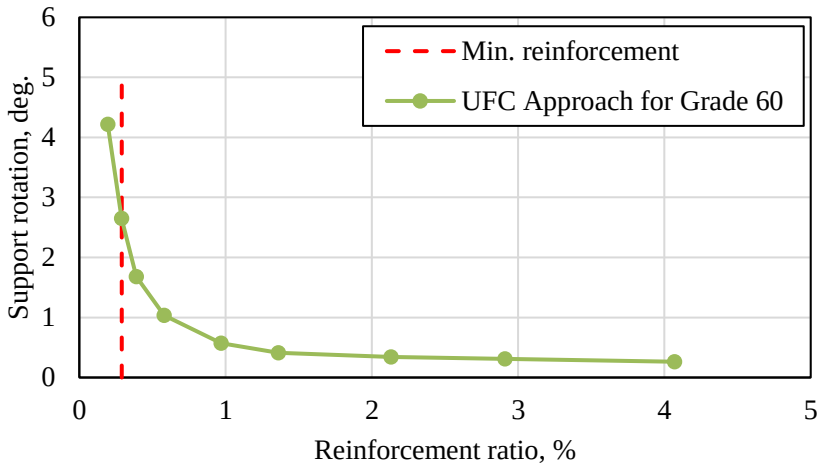

Figure 10: Support rotation versus reinforcement ratio for grade 60 steel

3.1 Computational model validation

The computational model is validated with experimental results adopted by Li and Aoude (2019) [6]. This study performed a static test on a simply supported beam with a span length of 87.87 in. The beam is subjected to two points loading located at 29.17 in. from supports and has a rectangular cross-section with 4.92 in. width and 9.84 in. height. The main reinforcement for the beam consisted of 2 No. 4 of ASTM A1035 bars. The beam has a cover of 1.38 in. The material properties for concrete and steel are shown in Table 1, where E_c is the modulus of elasticity for concrete and f_u is the ultimate stress for steel.

Table 1: Material properties of experimental specimen used for computational model validation

Experiment	Concrete		Steel		
	E_c, ksi	$f'c$, ksi	E_s, ksi	f_y, ksi	f_u, ksi
Li and Aoude (2019) [6]	5729.00	13.98	29000.00	131.11	156.21

Figure 11 shows the load displacement for both the computational model and the experiment. The results show generally good agreement. The computational model overestimates the experimental results with major variation at the middle range of displacement. This could be attributed to the type of model used to describe the concrete, where the concrete stress-strain test in the experimental study illustrated almost linear line up to the ultimate compressive strength, while the selected concrete model in this study has a curvature behavior, as shown in Figure 3. However, the model predicts well the maximum capacity and to some extent the initial stiffness.

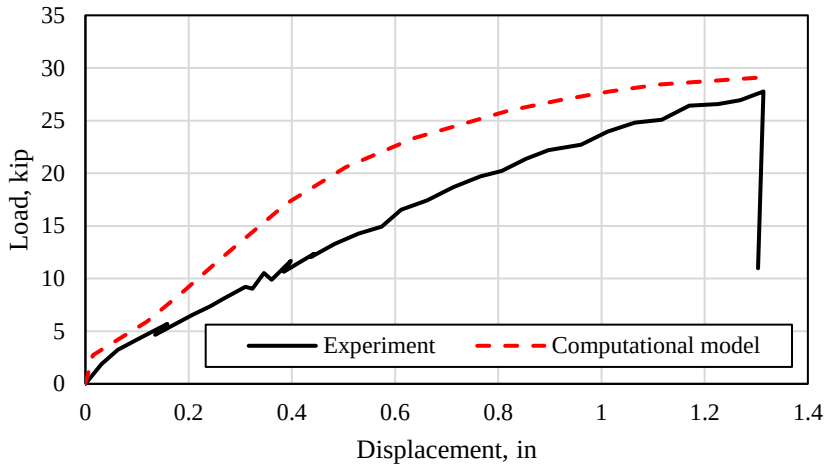

Figure 11: Computational model validation of load-displacement with Li and Aoude (2019) [6]

3.2 Feasibility of using the UFC approach for grade 100 steel

The UFC approach considers a simplified resistant function when analyzing a blast-resistant reinforced concrete flexural member. Steel strength is considered to be constant and equal to the yield strength when steel strain exceeds the yield point; in other words, it possesses a bi-linear curve. The UFC approach is investigated for a reinforced concrete member using grade 100 steel. A comparison was established between the computational model performance, which presents an actual response, and the UFC approach. The comparison focuses on the results within the minimum and maximum limits of the steel reinforcement ratios that have been required by (ACI 318-19) [19].

Figure 12 shows that the UFC approach resulted in higher values than the computational model approach when the reinforcement ratio is below 0.4%, while lower or equal values of the UFC approach than computational model results were observed when the reinforcement ratio is higher than 0.4%. This result illustrates that using the UFC approach to analyze a reinforced concrete member using grade 100 steel when subjected to the examined blast load may require adjustments when the reinforcement ratio is between 0.4% and 2% in order to reach conservative results. Adjustment may not be required elsewhere, as it can be noticed when the reinforcement ratio is higher than 2%, where the UFC and computational model approached almost similar results.

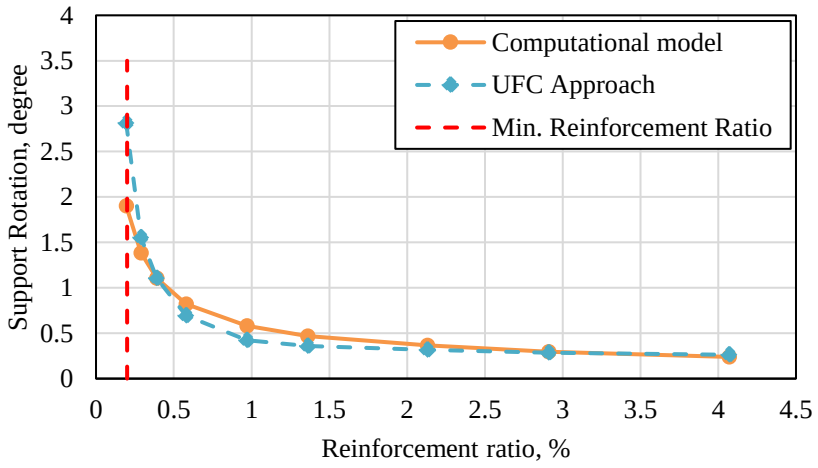

Figure 12: Computational model and the UFC approaches for grade 100

3.2 Performance comparison of grade 100 and grade 60 steels

This part illustrates the performance when using grade 100 steel as a reinforcement in a reinforced concrete flexural member instead of conventional steel (i.e., grade 60). A plot of support rotation versus reinforcement ratio for the computational model for grade 100 and grade 60 was provided (Figure 13). The plot shows that grade 100 and grade 60 steels show insignificant variation in support rotation performance when the reinforcement ratio is higher than 1.3%. The support rotation values, however, vary for reinforcement ratios less than 1.3%.

Table 2 shows a comparison when using rebar no. 4 steel of grade 100 instead of grade 60 steel for support rotation of 1.5 and 2 degrees. The amount of steel rebar was reduced nearly to half, which indicates less congestion in steel configuration in the cross-section and may result in less labor cost and reduced construction time.

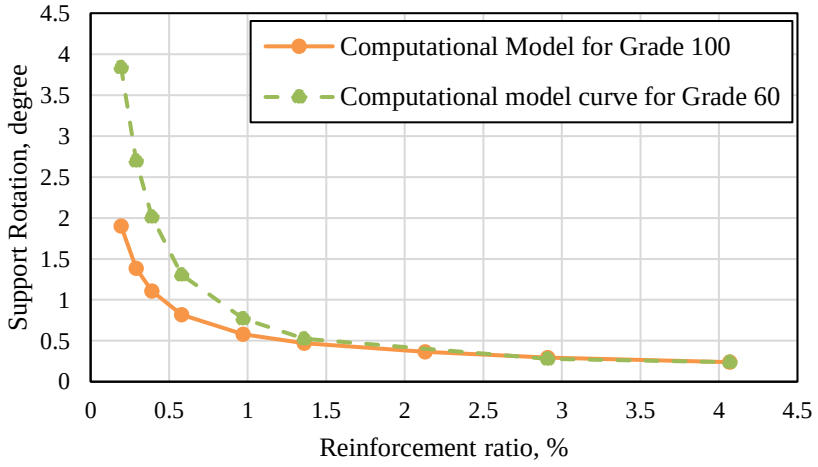

Figure 13: Computational model approach for grade 100 and grade 60

Table 2: Comparing the use of no. 4 steel bar of grade 100 and grade 60 steel

Support rotation	Type	Reinforcement ratio, %	Area, in^2	Number of rebars
1.5 degrees	Grade 100	0.27	0.7	7
	Grade 60	0.53	1.4	13
2 degrees	Grade 100	0.19	0.5	5
	Grade 60	0.39	1.0	10

4. Conclusions

In this study, simply supported rectangular cross-section flexural concrete members with double reinforcement were subjected to a blast load. The study examined a range of reinforcement ratios, i.e., 0.194 to 4.07%. The applied blast load was a simplified triangular load with 200 psi peak pressure and 10 msec duration. Two types of reinforcements are used: ASTM A1035 Grade 100 steel and conventional grade 60 reinforcement. The study investigated the UFC approach (the simplified approach), which is typically used during blast design stages to assess the performance of the flexural members with high strength reinforcements. The UFC approach simplifies the resistance function of the system to elastic-perfectly plastic. The study also compared the SDOF response of the UFC approach with a computational model that utilized a more realistic resistance-deflection function for the system. The study indicated a 50% reduction in the amount of steel when using grade 100 reinforcement instead of grade 60. This reduction indicates less steel congestion in the cross-section. The analysis concludes that employing the UFC approach yielded non conservative results within the reinforcement ratio between 0.4% and 2%. Hence, enhancing the UFC approach may be necessary to ascertain its reliability when designing for blast-resistant flexural members with ASTM A1035 Grade 100 steel. To make a comprehensive judgment, further investigations can be performed, which may include various blast regimes, boundary conditions, level of protections, reinforcement ratios, compressive strengths, and geometrical configurations.

5. References

[1] A01 Committee. Specification for Deformed and Plain, Low-Carbon, Chromium, Steel Bars for Concrete Reinforcement. ASTM International; n.d. https://doi.org/10.1520/A1035_A1035M-20.

[2] Mast RF, Dawood M, Rizkalla SH, Zia P. Flexural Strength Design of Concrete Beams Reinforced with High-Strength Steel Bars. SJ 2008;105:570–7. https://doi.org/10.14359/19940.

[3] Shahrooz BM, Reis JM, Wells EL, Miller RA, Harries KA, Russell HG. Flexural Members with High-Strength Reinforcement: Behavior and Code Implications. Journal of Bridge Engineering 2014;19:04014003. https://doi.org/10.1061/(ASCE)BE.1943-5592.0000571.

[4] Aldabagh S, Alam MS. High-Strength Steel Reinforcement (ASTM A1035/A1035M Grade 690): State-of-the-Art Review. Journal of Structural Engineering 2020;146:03120003. https://doi.org/10.1061/(ASCE)ST.1943-541X.0002720.

[5] Puranam AY. Strength and Serviceability of Concrete Elements Reinforced with High-Strength Steel. 2018.

[6] Li Y, Aoude H. Blast response of beams built with high-strength concrete and high-strength ASTM A1035 bars. International Journal of Impact Engineering 2019;130:41–67. https://doi.org/10.1016/j.ijimpeng.2019.02.007.

[7] Li Y, Aoude H. Effects of detailing on the blast and post-blast resilience of high-strength steel reinforced concrete (HSS-RC) beams. Engineering Structures 2020;219:110869. https://doi.org/10.1016/j.engstruct.2020.110869.

[8] ACI Committee 439. 439.6R-19: Guide for the Use of ASTM A1035/A1035M Type CS Grade 100 (690) Steel Bars for Structural Concrete. Technical Documents 2019.

[9] American Association of State Highway and Transportation Officials, editor. LRFD bridge design specifications. 9th edition. Washington, DC: American Association of State Highway and Transportation Officials; 2020.

[10] Keenan WA. BLAST LOADING OF CONCRETE BEAMS REINFORCED WITH HIGH-STRENGTH DEFORMED BARS,. 1963.

[11] Miyamoto A, King ME, Fujii M. Non-linear dynamic analysis and design concepts for RC beams under impulsive loads. BNZSEE 1989;22:98–111. https://doi.org/10.5459/bnzsee.22.2.98-111.

[12] Thiagarajan G, Kadambi AV, Robert S, Johnson CF. Experimental and finite element analysis of doubly reinforced concrete slabs subjected to blast loads. International Journal of Impact Engineering 2015;75:162–73. https://doi.org/10.1016/j.ijimpeng.2014.07.018.

[13] Li J, Wu C, Hao H. An experimental and numerical study of reinforced ultra-high performance concrete slabs under blast loads. Materials & Design 2015;82:64–76. https://doi.org/10.1016/j.matdes.2015.05.045.

[14] Department of Defense (DoD). UFC 3-340-02 Unified Facilities Criteria: Structures to Resist the Effects of Accidental Explosions. Washington, D.C: 2014.

[15] US Army Corps of Engineers Protective Design Center. TR 06-08 Single Degree of Freedom Structural Response Limits for Antiterrorism Design. Washington, DC: 2008.

[16] Biggs JM. Introduction to Structural Dynamics. McGraw-Hill, Inc.; 1964.

[17] Hibbeler RC. Structural analysis. 6th ed. Upper Saddle River, N.J: Pearson/Prentice Hall; 2006.
[18] Hognestad E. Inelastic Behavior in Tests of Eccentrically Loaded Short Reinforced Concrete Columns. JP 1952;49:117–39. https://doi.org/10.14359/11808.
[19] ACI Committee 318. ACI 318-19: Building Code Requirements for Structural Concrete and Commentary. Farmington Hills, MI: American Concrete Institute; 2019.

فحص أداء عناصر الإنحناء الخرسانية المحملة للإنفجار والمسلحة بقضبان عالية القوة

عمر العواد

قسم الهندسة المدنية- كلية الهندسة- جامعة القصيم- المملكة العربية السعودية

omar.awwad@qu.edu.sa

ملخص البحث. تبحث هذه الدراسة في استخدام حديد التسليح عالي القوة (ASTM A1035 Grade 100) بدلاً من التسليح التقليدي (مثل ASTM A615 Grade 60) في عناصر الإنحناء الخرسانية المسلحة والمقاومة للإنفجار. يختلف منحنى الإجهاد والانفعال للحديد ASTM A1035 Grade 100 عن الحديد التقليدي من الدرجة 60. يمتلك الحديد من الدرجة 100 قوة أعلى وحد خضوع غير واضح. عند تصميم عنصر الإنحناء الخرساني المسلح لمقاومة أحمال الانفجار، يتم احتساب المقاومة الخاصة به عادةً باستخدام دليل (UFC 3-340-02). تعمل منهجية UFC على تبسيط سلوك حديد التسليح إلى جزء مرن يصل إلى نقطة الخضوع، يليه عدم تغيرمثالي للمقاومة. مع عدم وجود نقطة خضوع واضحة في الحديد عالي القوة، قد لا يتم تمثيل هذا التبسيط بشكل جيد. الأداء الديناميكي للعناصر الخرسانية المرنة والمقواة بجديد التسليح عالي القوة عادة يتم احتسابها باستخدام نظام درجة الحرية الواحدة (SDOF). الدراسة قامت بمقارنة أداء SDOF الناتج من الطريقة المبسطة بطريقة تطور المقاومة لتكون أكثر واقعية و التي تم الحصول عليها بواسطة نموذج حسابي تم إنشاؤه باستخدام مبدأ الشغل الافتراضي و علاقة العزم-الانحناء للقطاع. أشارت النتائج إلى أن استخدام طريقة UFC للعناصر التي تحتوي على حديد التسليح عالي القوة قد يتطلب عامل تعديل من أجل الوصول إلى توقعات متحفظة عندما تكون نسبة التسليح بين 0.4% و2%. أوضحت النتائج أيضًا انخفاضًا بنسبة 50٪ في مساحة حديد التسليح عند استخدام درجة 100 بدلاً من درجة 60، مما يشير إلى تقليل احتقان حديد التسليح في العناصر المسلحة بحديد عالي القوة.